XLIII CILAMCE
21-25, November, 2022
FOZ DO IGUAÇU - PR - BRAZIL

Solution of ill-posed problem in plane wave decomposition for sound field reconstruction

Augusto C. F. de Carvalho[1], Hilbeth P. A. de Deus[1], Márcio H. A. Gomes[2], Eric Brandão[3], Lorenzo F. R. Garron[4]

[1]*Postgraduate Program in Mechanical and Materials Engineering, Federal University of Technology of Paraná*
Rua Deputado Heitor Alencar Furtado, 5000, Cidade Industrial de Curitiba, 81280-340, Curitiba/Paraná, Brazil
augustoc@alunos.utfpr.edu.br, azikri@utfpr.edu.br
[2]*Academic Department of Mechanics, Federal University of Technology of Paraná*
Rua Deputado Heitor Alencar Furtado, 5000, Cidade Industrial de Curitiba, 81280-340, Curitiba/Paraná, Brazil
marciogomes@utfpr.edu.br
[3]*Acoustic Engineering, Federal University of Santa Maria*
Avenida Roraima, 1000, Camobi, 97105-900, Santa Maria/Rio Grande do Sul, Brazil
eric.brandao@eac.ufsm.br
[4]*Mechatronics Engineering, Federal University of Technology of Paraná*
Rua Deputado Heitor Alencar Furtado, 5000, Cidade Industrial de Curitiba, 81280-340, Curitiba/Paraná, Brazil
lgarron@alunos.utfpr.edu.br

Abstract. Plane-wave decomposition is a recently developed technique in the field of acoustics that stems from an approximation in the inverse spatial tri-dimensional Fourier transform so that it considers that the sound field is represented by the superposition of plane waves traveling in well-defined directions. The calculations for the technique involve the solution of an ill-posed matrix equation, requiring a regularized solution for the least squares problem. This paper will show the implementation of the plane wave decomposition using Tikhonov regularization in the context of a simulated and a measured impedance tube. The classical L-curve algorithm and a fixed-point algorithm for the calculation of the regularization parameter were investigated and compared with the goal of defining which technique produces the least error in this scenario. The reconstructions of the transfer functions in both the simulated case and the measured case were realised, with the fixed-point algorithm displaying an advantage over the L-curve with respect to reconstruction errors in both scenarios.

Keywords: room acoustics, inverse problems, plane wave decomposition, virtual microphone array, sound field reconstruction

1 Introduction

The wavenumber approach is a technique that allows to decompose a sound field in components represented by plane waves, from pressure or transfer function measurements of different points in space. The method, initially proposed by Nolan [1], relies on a discretization of a spherical spatial Fourier transform, which in turn leads to an ill-posed matrix equation. The non-existence of an inverse matrix makes so that a regularization is needed to find an approximate solution. An interesting case to test the technique is the impedance tube. Because of its dimensions, an impedance tube can be considered (inside a certain frequency range) as only having a plane wave emitted by the speaker and a plane wave reflected by an absorbing sample or rigid cap. Furthermore, the impedance tube has a limited amount of positions in which a microphone can sample the sound field. Thus, this paper will explore the possibility of the reconstruction of the transfer functions of the tube using the wavenumber approach. Moreover, a comparison between the reconstruction errors of two regularization parameter techniques (the L-curve algorithm [2] and the fixed point algorithm [3, 4]) was done.

2 Theoretical Fundamentals

This section presents concepts, ideas and techniques that are useful to understand the contents of this paper.

2.1 Plane-wave decomposition and the wavenumber spectrum

Plane-wave decomposition is a technique that stems from the discretization of a spherical inverse Fourier transform. According to Nolan [1], the spherical Fourier transform is

$$p(\mathbf{r}_m) = \iiint\limits_{-\infty}^{+\infty} P(\mathbf{k})\mathrm{e}^{-\mathrm{j}\langle \mathbf{k},\mathbf{r}\rangle}\,\mathrm{d}\mathbf{k}, \tag{1}$$

where $p(\mathbf{r}_m) \in \mathbb{C}$ is the sound pressure at a spatial position $\mathbf{r}_m \in \mathbb{R}^3$, $\mathbf{k} \in \mathbb{R}^3$ is the wavenumber vector, and $P(\mathbf{k}) \in \mathbb{C}$ is the wavenumber spectrum. Notice that $\langle \mathbf{k}, \mathbf{r}\rangle$ denotes the inner product between $\mathbf{r}$ and $\mathbf{k}$. The wavenumber spectrum $P(\mathbf{k})$ as a complex quantity and can be written as

$$P(\mathbf{k}) = |P(\mathbf{k})|\,\mathrm{e}^{\mathrm{j}\,\phi(\mathbf{k})}, \tag{2}$$

where $|P(\mathbf{k})|$ is the absolute value and $\phi(\mathbf{k})$ are the modulus and the phase of the complex value $P(\mathbf{k})$.

The first hypothesis that Nolan [1] presents to derive eq. (1) further is that $\|\mathbf{k}\|^2 = k_x^2 + k_y^2 + k_z^2$ such that $\|\mathbf{k}\|^2 \geq k_x^2 + k_y^2$, which means that no evanescent waves i.e. waves that do not radiate to the far field are present. Equation (1) can be written in spherical coordinates through the following changes of variables: $x_m = r\sin(\gamma)\cos(\xi)$, $y_m = r\sin(\gamma)\sin(\xi)$, $z_m = r\cos(\gamma)$, $k_x = k\sin(\theta)\cos(\phi)$, $k_y = k\sin(\theta)\sin(\phi)$, $k_z = k\cos(\theta)$; which leads to eq. (3)

$$p(\mathbf{r}_m) = \int\limits_0^{+\infty}\int\limits_0^{2\pi}\int\limits_0^{\pi} P(\mathbf{k})\mathrm{e}^{-\mathrm{j}\,k\,r\,(\sin(\gamma)\sin(\theta)\cos(\phi-\xi)+\cos(\theta)\cos(\gamma))}\,k^2\sin(\theta)\,\mathrm{d}k\,\mathrm{d}\theta\,\mathrm{d}\phi, \tag{3}$$

where $p(\mathbf{r}_m) = p(r,\gamma,\xi)$ in the spherical coordinates of the space and $P(\mathbf{k}) = P(k,\theta,\phi)$ in the spherical coordinates of the *k-space* (Remark 2). At this moment, the sound field can be considered as produced by a pure-tone with a single excitation frequency f_0, which according to Nolan [1] implies that propagating waves are all existing in the surface of a radiation sphere in the wavenumber domain. This radiation sphere has radius equal to $k_0 = (2\pi f_0)/c$,
where k_0 is the radius of the radiation sphere, f_0 is the pure-tone frequency, and c is the speed of sound. In that case, Nolan [1] asserts that the sound field in the wavenumber domain can be written as

$$P(k,\theta,\phi) = \frac{\delta(k-k_0)}{4\pi k^2}\widetilde{P}(\theta,\phi), \tag{4}$$

where $\delta(k-k_0)/4\,\pi\,k^2$ is the spherical Dirac delta function for spherically symmetric curved spaces and $\widetilde{P}(\theta,\phi)$ is the two-dimensional wavenumber spectrum. Substituting eq. (4) into eq. (3), and noting that $\delta(k-k_0) = 1$ only when $k = k_0$, the sound pressure field can be written as

$$p(\mathbf{r}_m) = \frac{1}{4\,\pi}\int\limits_0^{2\pi}\int\limits_0^{\pi} \widetilde{P}(\theta,\phi)\mathrm{e}^{-\mathrm{j}\,k_0\,r\,(\sin(\gamma)\sin(\theta)\cos(\phi-\xi)+\cos(\theta)\cos(\gamma))}\sin(\theta)\,\mathrm{d}\theta\,\mathrm{d}\phi. \tag{5}$$

Given the considerations of pure-tone excitation, eq. (5) proposes a bi-dimensional wavenumber spectrum, which can be interpreted as a linear combination of plane waves travelling in the direction (θ,ϕ) with wavenumber k related to the excitation frequency. In practical terms, Nolan [1] implements a discrete approximation of eq. (5)

$$p(\mathbf{r}_m) = \sum_{l=1}^{L}\widetilde{P}(\mathbf{k}_l)\mathrm{e}^{-\mathrm{j}\langle \mathbf{k}_l,\mathbf{r}_m\rangle}, \tag{6}$$

where the variables have the same meaning as in eq.(1), with the addition of the index $l = 1, ..., L$, which leads to the wavenumber vectors $\{\mathbf{k}_1, ..., \mathbf{k}_l, ..., \mathbf{k}_L\}$, distributed uniformly over the k-space. In the same sense, $m = 1, ..., M$ leads to a discrete quantity of points in the physical space of the room $\{\mathbf{r}_1, ..., \mathbf{r}_m, ..., \mathbf{r}_M\}$. It is worth remarking that eq. (6) is valid for the sound pressure in a certain receiver in a position. Denoting, as Nolan [1] does, $\psi_l(\mathbf{r}_m) = \mathrm{e}^{-\mathrm{j}\langle \mathbf{k}_l, \mathbf{r}_m \rangle}$, and $\widetilde{P}(\mathbf{k}_l) = x_l$, the sampling of the sound field in many positions can be written as a matrix equation

$$\mathbf{p} = H\,\mathbf{x}, \tag{7}$$

where $\mathbf{p} \in \mathbb{C}^M$ is a vector with the sound pressure sampled in the positions $\{\mathbf{r}_1, ..., \mathbf{r}_m, ..., \mathbf{r}_M\}$, $\mathbf{x} \in \mathbb{C}^L$ is a vector containing the bi-dimensional wavenumber spectrum related to the directions $\{\mathbf{k}_1, ..., \mathbf{k}_l, ..., \mathbf{k}_L\}$. The matrix $H \in \mathbb{C}^{M \times L}$ is usually called *sensing matrix* and has elements $\psi_{m,l}(\mathbf{r}_m, \mathbf{k}_l) = \mathrm{e}^{-\mathrm{j}\langle \mathbf{k}_l, \mathbf{r}_m \rangle}$. The sensing matrix is usually rectangular, which leads to an ill-posed problem. Thus, to find $\mathbf{x}$ from a set of measurements $\mathbf{p}$, regularization techniques are needed.

To reconstruct the sound pressures at a different set of positions knowing the wavenumber spectrum $\mathbf{x}$, it is enough to solve the problem described by eq. (7) using an appropriate sensing matrix H i.e. its components $\psi_{m,l}(\mathbf{r}_m, \mathbf{k}_l)$ should be calculating for the reconstruction positions.

2.2 Tikhonov regularization

To compute the wavenumber spectrum by means of eq. (7), the first instinct is to find the inverse matrix of H. However, as stated in Remark 3, H is usually rectangular and thus H^{-1} does not exist. This means usually that there will be infinite possible solutions $\mathbf{x}$ for eq. (7) with a given $\mathbf{p}$. Then, the first alternative is to solve a least squares problem with formulation

$$\hat{\mathbf{x}} = \min_x \|H\,\mathbf{x} - \mathbf{p}\|_2^2, \tag{8}$$

where $\|\cdot\|_2^2$ denotes the square of the Euclidean norm. However, given the physical interpretation attached to the solution $\mathbf{x}$, the solution to the problem in eq. (8) might not be the most appropriate for the phenomena that are being analysed. On that account, finding a more correct solution requires the employment of a regularization to the least squares problem, which essentially means specifying a restriction that the solution should be fit to. The choice of regularization technique depends on the type of environment being analysed. Nolan [1] relates a couple of cases to certain types of regularization. The most common and most versatile technique is the Tikhonov regularization, which Nolan [1] cites as being very much appropriate to reverberant or fairly reverberant rooms. It also has been deemed appropriate for *in situ* sound field evaluations such as in the experiments conducted by Nolan [1] and for *in situ* absorption evaluation by Nolan [5] and Carvalho [6].

The Tikhonov regularization is defined by Hansen [2] as

$$\hat{\mathbf{x}} = \min_x \|H\,\mathbf{x} - \mathbf{p}\|_2^2 + \lambda^2\,\|x\|_2^2 = \min_x \langle H\,\mathbf{x} - \mathbf{p},\, H\,\mathbf{x} - \mathbf{p}\rangle + \lambda^2\,\langle \mathbf{x}, \mathbf{x}\rangle, \tag{9}$$

in which λ is called regularization parameter and it is what ponders between the norm of the residual $\|H\,\mathbf{x} - \mathbf{p}\|_2$ (how well the solution fits the problem) and the norm of the solution $\|x\|_2$. Excessively large values of λ will produce small norm solutions that don't fit the problem very well, and, conversely, excessively small values of λ will produce less regular solutions.

Knowing that the point of minimum $\hat{\mathbf{x}}$ happens when the derivative of the expression equals 0 leads to an equation where $\hat{\mathbf{x}}$ an be isolated, leading to

$$\hat{\mathbf{x}} = (H^*\,H + \lambda^2\,\mathbb{I})^{-1}\,H^*\,\mathbf{p}. \tag{10}$$

Equation (10) can be further simplified by taking the singular value decomposition (SVD) of H. Knowingly, the SVD of a matrix can be written as $H = U\,\Sigma\,V^*$, where U and V are orthogonal (i.e. $U^{-1} = U^T$) and Σ is a diagonal matrix containing the singular values $\{\sigma_1, ..., \sigma_M\}$ of H in its principal diagonal. Thus the substitution of the SVD of H into eq. (10), and writing $\mathbb{I} = V\,V^*$ leads to

$$\hat{\mathbf{x}} = V\,(\Sigma^*\,\Sigma + \lambda^2\,\mathbb{I})^{-1}\,\Sigma^*\,U^*\,\mathbf{p}. \tag{11}$$

Equation (11) is still not the simplest form of solving the Tikhonov regularization, as matrix inversion is a rather cumbersome process in the computational sense. Having in mind the nature of U, V, and Σ, eq. (11) can be written as a summation of vectors

$$\hat{\mathbf{x}} = \sum_{i=1}^{n} \frac{\sigma_i^*}{|\sigma_i|^2 + \lambda^2}\,\mathbf{u}_i^*\,\mathbf{p}\,\mathbf{v}_i = \sum_{i=1}^{n} \frac{|\sigma_i|^2}{|\sigma_i|^2 + \lambda^2}\,\frac{\mathbf{u}_i^*\,\mathbf{p}}{\sigma_i}\,\mathbf{v}_i = \sum_{i=1}^{n} \Phi_i^{[\lambda]}\,\frac{\mathbf{u}_i^*\,\mathbf{p}}{\sigma_i}\,\mathbf{v}_i, \tag{12}$$

where $\Phi_i^{[\lambda]}$ is called filter factor by Hansen [2], and it behaves such that for comparatively small values of λ with relation to the singular values σ_i, $\Phi_i^{[\lambda]} = 1$ and for much larger values of λ, $\Phi_i^{[\lambda]} = \sigma_i^2/\lambda^2$. This "filtering" is interesting because it reduces the influence of the errors caused by the smaller singular values, as when $\lambda >> \sigma_i$ the term σ_i^2/λ^2 eventually forces errors in $\mathbf{u}_i$ and $\mathbf{v}_i$ to be smaller.

To use Tikhonov regularization, the parameter λ must be defined beforehand. This paper will explore two different techniques: the "L-curve technique" and the "fixed point iterations technique".

2.3 The L-curve technique

The L-curve method for determining the regularization parameter consists of pondering between the norm of the solution $\|\hat{\mathbf{x}}\|_2$ and the norm of the residue $\|H\,\hat{\mathbf{x}} - \mathbf{p}\|_2$. Their squares after substituting the SVD matrices are

$$\|\hat{\mathbf{x}}\|_2^2 = \sum_{i=1}^{n} \left(\Phi_i^{[\lambda]}\,\frac{\mathbf{u}_i^*\mathbf{p}}{\sigma_i}\right)^2, \tag{13}$$

and

$$\|H\,\hat{\mathbf{x}} - \mathbf{p}\|_2^2 = \sum_{i=1}^{n} \left((\Phi_i^{[\lambda]} - 1)\,\mathbf{u}_i^*\mathbf{p}\right)^2 + \varepsilon^2. \tag{14}$$

By analysing the derivatives of eq. (13) and eq. (14) in λ, Hansen [2] shows that both norms are monotone with relation to λ. Moreover, Hansen [2] goes further and shows that $\|\hat{\mathbf{x}}\|_2^2$ is a monotonically decreasing function of $\|H\,\hat{\mathbf{x}} - \mathbf{p}\|_2^2$. Hansen also derives the curvature of the function in λ that relates $\|\hat{\mathbf{x}}\|_2$ and $\|H\,\hat{\mathbf{x}} - \mathbf{p}\|_2$.

The idea behind the L-curve method is to find the parameter λ that produces the maximum curvature on the relation between $\|\hat{\mathbf{x}}\|_2$ and $\|H\,\hat{\mathbf{x}} - \mathbf{p}\|_2$. The curve is called L-curve because when plotted in logarithmic scales it has a shape similar to the letter "L". The maximum curvature spot is what determines a change in behaviour following increase in λ, as in the "vertical part" there's larger values of $\|\hat{\mathbf{x}}\|_2$ and smaller values of $\|H\,\hat{\mathbf{x}} - \mathbf{p}\|_2$, and vice-versa for the "horizontal part". Furthermore, the magnitude of λ is also related to the effect of perturbations in the solution. A small λ has a smaller residue, but its associated solution has more influence of noise. Conversely, larger values of λ display larger residues (so it has larger numerical error), but the solution is "smoother" and the influence of noise is mitigated. The point of maximum curvature is deemed to contain a value of λ that is a good ponderation between both cases.

2.4 The fixed point iteration technique

The fixed-point iterations technique was first proposed by Fermín [3], based on early work developed by Regińska [4]. It essentially consists of finding a local minimum of an auxiliary function, which relates to the point of maximum curvature in the L-curve.

Calling a certain Tikhonov solution for a generic parameter λ as $\mathbf{x}_\lambda$, $x(\lambda) = \|\mathbf{x}_\lambda\|_2$ and $y(\lambda) = \|H\,\mathbf{x}_\lambda - \mathbf{p}\|_2$, the auxiliary function $\Psi_\mu(\lambda)$ is defined

$$\Psi_\mu(\lambda) = x(\lambda)\, y(\lambda)^\mu, \tag{15}$$

where $\mu > 0$.

Regińska's [4] article presents proof that if λ^* maximizes the curvature of the L-curve, and if the tangent of the L-curve at the point $(\log(x(\lambda^*)), \log(y(\lambda^*)))$ has inclination $-1/\mu$, then λ^* minimizes Ψ_μ.

Fermín [3] proposes the minimization of Ψ_μ by means of eq. (16) (the derivative of Ψ_μ with relation to λ)

$$\Psi'_\mu(\lambda) = y(\lambda)^\mu\, y'(\lambda) \left(\frac{x'(\lambda)}{y'(\lambda)} + \mu \frac{x(\lambda)}{y(\lambda)} \right), \tag{16}$$

and the knowledge that $y(\lambda)^\mu\, y'(\lambda) \neq 0$ and $x'(\lambda)/y'(\lambda) = -\lambda^2$. When these facts are combined, the condition for $\Psi'_\mu(\lambda) = 0$ is that

$$(\lambda^*)^2 = \mu \frac{x(\lambda^*)}{y(\lambda^*)} \;\therefore\; \lambda^* = \sqrt{\mu}\, \frac{\sqrt{x(\lambda^*)}}{\sqrt{y(\lambda^*)}}. \tag{17}$$

To transform eq. (17) into a fixed-point problem i.e. a problem where $\varphi(\lambda^*) = \lambda^*$, it is enough to call

$$\varphi(\lambda) = \sqrt{\mu}\, \frac{\sqrt{x(\lambda)}}{\sqrt{y(\lambda)}}. \tag{18}$$

Fermín [3] attests that the criterion to find λ using the fixed-point problem is that the λ^* that minimizes Ψ_μ is near the corner of the L-curve in log-log scale. Moreover, the process does not depend on the μ value, so by process of iteration, if no minimum of Ψ_μ is found for a certain μ, its value can be changed, and the search for the minimum happens in a different function Ψ_μ.

3 Experiments and Simulations - Reconstruction of the Sound Field on an Impedance Tube

Impedance tubes are devices used to measure the normal incidence acoustic absorption. On this type of device, a speaker placed on one side of the tube creates an acoustic field in its interior. The other extremity of the tube is closed with a sample of the material to be characterised. Because of the dimensions of the tube, the sound field can be considered as composed by two plane-waves, one emitted by the speaker and the reflection off the absorbing sample for a range of frequency [7].

The transfer function in the impedance tube between the pressure in a point a certain length z from the sample at the termination and the sound source, according to Jacobsen and Juhl [8], is given by

$$F(z) = \frac{p(z)}{p_s(z_s)} = \frac{(\mathrm{e}^{-\mathrm{j}kz} - R\,\mathrm{e}^{\mathrm{j}kz})}{(\mathrm{e}^{-\mathrm{j}kz_s} - R\,\mathrm{e}^{\mathrm{j}kz_s})}. \tag{19}$$

where p is the sound pressure in a distance z from the source, p_s is the sound pressure at the source, k is the wavenumber of the oscillation $k = (2\pi f)/c$, and R is the reflection coefficient of the sample surface. The term $\mathrm{e}^{\mathrm{j}\omega t}$, which represents the time dependence, can be omitted.

The impedance tube used for these experiments was designed by Busulo [9]. It has three slots for the transducer, which will form the sequential measurement array. The impedance tube has a frequency range between 200 Hz and 2700 Hz The measurements and simulations were done as part of the work produced by Garron [10].

The simulated transfer function for a tube with a $R = 0.85$ (green dotted line) and the reconstructions for the position 3 using the L-curve (blue dashed line) and the fixed point (maroon dashed line) algorithms are displayed in Fig. 1a. The measured transfer function for Busulo's tube [9] (green dotted line) and the reconstructions for the position 3 using the L-curve (blue dashed line) and the fixed point (maroon dashed line) algorithms are displayed in Fig. 1b.

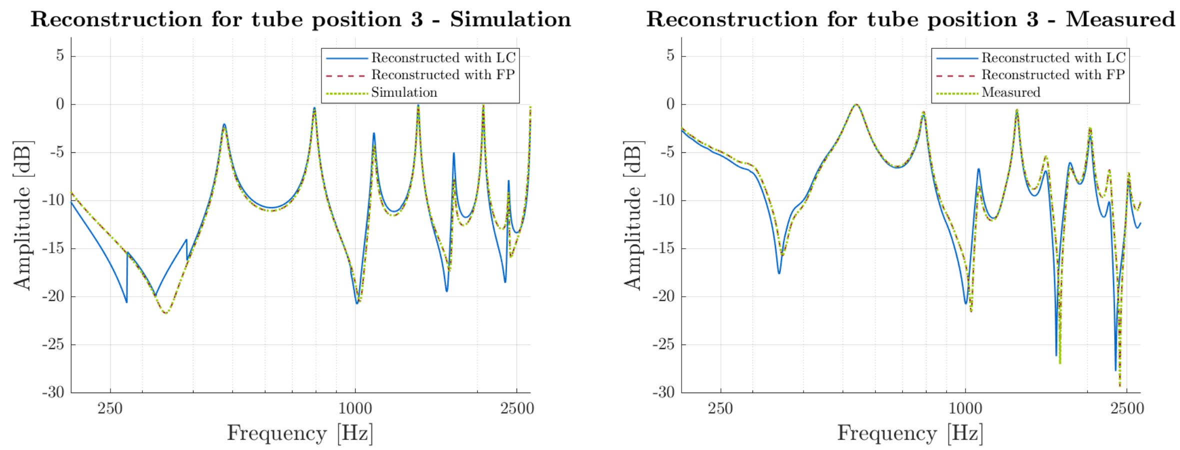

(a) Simulated transfer function.

(b) Measured transfer function.

Figure 1. Simulated (a) and measured (b) transfer functions and reconstructions for position 3 of the impedance tube.

In Fig. 1 it can be seen that the reconstruction using the fixed point regularization parameter produces a reconstruction more coherent than the reconstruction using the L-curve algorithm, for either the simulated or measured transfer functions. The average relative percentage errors for each third-of-octave bands for the simulation (Fig. 2a) and for the measurement (Fig. 2b) are displayed in Fig. 2. The calculation of the relative error follows the metric proposed by de Carvalho et al. [6]. The blue asterisks are the L-curve errors and the maroon asterisks are the fixed point errors, with the dashed lines added to avoid parallax. The error was averaged in the three transducer positions.

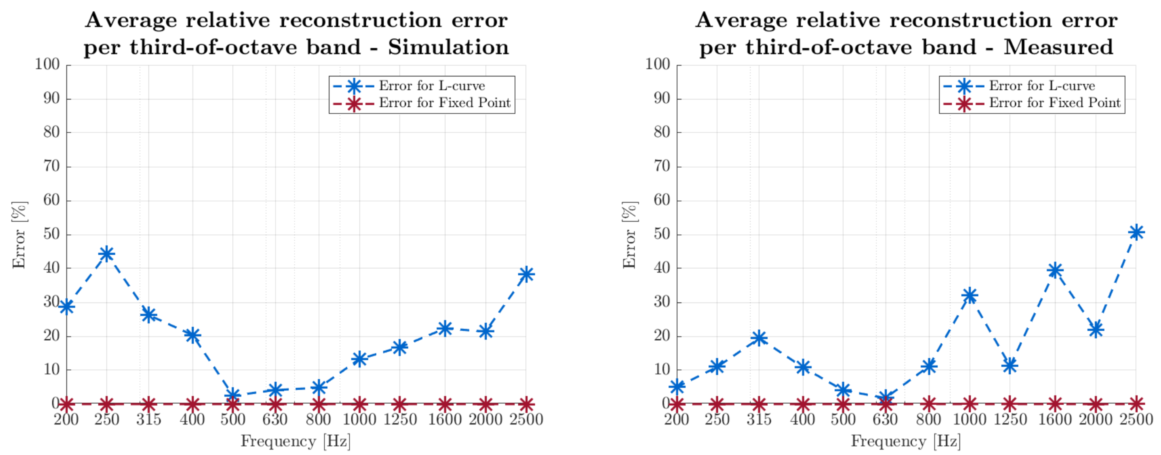

(a) Simulation.

(b) Measurement.

Figure 2. Simulated (a) and measured (b) third-of-octave average reconstruction error for position 3 of the impedance tube.

Figure 2 makes it evident that the fixed point regularization parameter causes reconstruction errors of smaller significance than the ones on the L-curve case. This happens most likely for a few reasons. For starters, the wavenumber spectrum for the impedance tube does not have the same requirement for smoothness (or regularity) as the one for strongly reverberant [1] or common rooms [6]. As such, the choice of smaller regularization parameters is sufficient to provide a reliable reconstruction of the sound field.

Another factor that may influence the quality of the regularized solution is the condition number of the sensing matrix. For larger sensing matrices i.e. for more sampling positions or for a more refined decomposition, the condition number tends to increase. The increase in the sensing matrices' condition numbers can, in turn, increase numerical errors in the regularization.

Another observation that can be made about 2 is the existence of discontinuities on the transfer function reconstructed using L-curve on the simulated scenario. This may be related to the L-curve not being able to find a regularized solution that fits the simulation without noise which can be interpreted as a stricter constraint than the measured case. Again, this is not a problem for the fixed-point algorithm. Furthermore, for the L-curve errors, a behaviour similar to the one found in the regularization problem for the transfer function reconstruction in a room [6], in which there's a rise on the reconstruction errors for the higher frequencies and the lower frequencies, with a middle band in which the error is lower.

4 Conclusions

The wavenumber spectrum was calculated from three samples of the sound field for a simulation and for a real measurement in an impedance tube. The transfer functions for each of the measurement points were reconstructed. The average relative errors between reconstructions and measurements were computed and averaged in the positions and then in third-of-octave bands. The regularization using the fixed point parameter achieved smaller errors than the L-curve parameter. The behaviour of the errors for the L-curve follows the expected for the method. Ideas for future works include the assessment of the condition number for the sensing matrices and their relation to the reconstruction error, the inclusion of noise in the simulation, and exploring the potential of calculating normal incidence absorption using the wavenumber approach.

Acknowledgements. The authors would like to thank the National Research Council of Brazil (CNPq - *Conselho Nacional de Desenvolvimento Científico e Tecnológico*; *Projeto Universal*: n° 402633/2021-0) and the Coordination for the Improvement of Higher Education Personnel (CAPES - *Coordenação de Aperfeiçoamento de Pessoal de Nível Superior*; CAPES-DS grant: n° 88887.644633/2021-00) for the partial financial support to this research paper.

Authorship statement. The authors hereby confirm that they are the sole liable persons responsible for the authorship of this work, and that all material that has been herein included as part of the present paper is either the property (and authorship) of the authors, or has the permission of the owners to be included here.

References

[1] M. Nolan. *Experimental characterization of the sound field in a reverberation room*. PhD thesis, Technical University of Denmark, 2019.

[2] P. C. Hansen. *Discrete Inverse Problems*. SIAM, Philadelphia, United States of America, 1 edition, 2010.

[3] F. S. V. Bazán. Fixed-point iterations in determining the tikhonov regularization parameter. *Inverse Problems*, vol. 24, 2008.

[4] T. Regińska. A regularization parameter in discrete ill-posed problems. *SIAM Journal on Scientific Computing*, vol. 17, 1996.

[5] M. Nolan. Estimation of angle-dependent absorption coefficients from spatially distributed in situ measurements. *The Journal of the Acoustical Society of America*, vol. 147, pp. 119–124, 2020.

[6] A. C. F. de Carvalho, M. H. A. Gomes, E. Brandão, H. P. A. de Deus, and L. P. Laus. Application of wavenumber approach for room behaviour analysis and absorption coefficient measurement. Florianópolis, Brazil. 12th Ibero-american Acoustics Congress, 2022.

[7] E. Brandão. *Acústica de Salas*. Blucher, São Paulo, São Paulo, 2016.

[8] F. Jacobsen and P. M. Juhl. *Fundamentals of General Linear Acoustics*. Wiley, Chichester, United Kingdom, 2013.

[9] W. F. Busulo. Construção de um tubo de impedâncias e teste através do método de função de transferência. Diploma thesis, Federal University of Technology of Paraná, 2017.

[10] L. F. R. Garron. Abordagem de problemas inversos em movimentos ondulatórios: Reconstrução de campo sonoro. Diploma thesis, Federal University of Technology of Paraná, 2022.